Published in final edited form as:
Free Radic Biol Med. 2011 October 15; 51(8): 1492–1500. doi:10.1016/j.freeradbiomed.2011.07.004.

Role of VPO1, a newly identified heme-containing peroxidase, in ox-LDL induced endothelial cell apoptosis

Yong-Ping Bai[a,c,1], **Chang-Ping Hu**[b,1], **Qiong Yuan**[b], **Jun Peng**[b], **Rui-Zheng Shi**[a], **Tian-Lun Yang**[a], **Ze-Hong Cao**[d], **Yuan-Jian Li**[b], **Guangjie Cheng**[d,*], and **Guo-Gang Zhang**[a,*]

[a]Department of Cardiovascular Medicine, Xiangya Hospital, Central South University, Changsha, 410008, China

[b]Department of Pharmacology, School of Pharmaceutical Sciences, Central South University, Changsha 410078, China

[c]Department of Geriatric Medicine, Xiangya Hospital, Central South University, Changsha, 410008, China

[d]Division of Pulmonary, Allergy & Critical Care Medicine, Department of Medicine, University of Alabama at Birmingham, Birmingham, AL 35294, USA

Abstract

Myeloperoxidase (MPO) is an important enzyme involved in the genesis and development of atherosclerosis. Vascular peroxidase 1 (VPO1) is a newly discovered member of the peroxidase family that is mainly expressed in vascular endothelial cells and smooth muscle cells and has structural characteristics and biological activity similar to those of MPO. Our specific aims were to explore the effects of VPO1 on endothelial cell apoptosis induced by oxidized low-density lipoprotein (ox-LDL) and the underlying mechanisms. The results showed that ox-LDL induced endothelial cell apoptosis and the expression of VPO1 in endothelial cells in a concentration- and time-dependent manner concomitant with increased intracellular reactive oxygen species (ROS) and hypochlorous acid (HOCl) generation, and up-regulated protein expression of the NADPH oxidase $gp91^{phox}$ subunit and phosphorylation of p38 MAPK. All these effects of ox-LDL were inhibited by VPO1 gene silencing and NADPH oxidase $gp91^{phox}$ subunit gene silencing or by pretreatment with the NADPH oxidase inhibitor apocynin or diphenyliodonium. The p38 MAPK inhibitor SB203580 or the caspase-3 inhibitor DEVD-CHO significantly inhibited ox-LDL-induced endothelial cell apoptosis, but had no effect on intracellular ROS and HOCl generation or the expression of NADPH oxidase $gp91^{phox}$ subunit or VPO1. Collectively, these findings suggest for the first time that VPO1 plays a critical role in ox-LDL-induced endothelial cell apoptosis and that there is a positive feedback loop between VPO1/HOCl and the now-accepted dogma that the NADPH oxidase/ROS/p38 MAPK/caspase-3 pathway is involved in ox-LDL-induced endothelial cell apoptosis.

Keywords

VPO1; MPO; NADPH oxidase; Apoptosis; Endothelial cells; Free radicals

*Corresponding authors. Fax: +1 086 731 84327695; +1 205 935 8565. gjcheng@uab.edu (G. Cheng), xyzgg2006@sina.com (G.-G. Zhang).

[1]These two authors contributed equally to this work.

To clarify the source of reactive oxygen species (ROS), and subsequently to remove ROS, is one of the important measures in preventing atherosclerosis. Myeloperoxidase (MPO) has been implicated in the initiation and progression of atherosclerotic plaques [1,2]. MPO catalyzes a reaction between hydrogen peroxide and chloride to generate potent oxidants, including hypochlorous acid (HOCl), while reacting with nitric oxide and nitrite to produce reactive nitrating species [3]. MPO and its oxidant by-products are detected in atherosclerotic lesions, colocalizing with foam cell macrophages, and are especially abundant at sites of thrombosis, suggesting that MPO oxidants destabilize vulnerable plaques [1,4]. MPO oxidizes low-density lipoprotein (LDL) to create a more atherogenic form taken up more effectively by macrophage scavenger receptors, generating foam cells [5]. MPO further enhances foam cell formation by oxidizing ApoA1, the major protein component of high-density lipoprotein, impairing ABCA-1-mediated cholesterol efflux from foam cells [6–8]. In addition, MPO scavenges nitric oxide, inhibits the expression of nitric oxide synthase, and consequently impairs vasodilation [9].

Higher levels of MPO gene expression are linked to increased risk of atherosclerosis [10]. A functional MPO promoter polymorphism, –463 G/A, is associated with increased incidence of coronary artery disease (CAD) and severity of atherosclerosis [11]. The –463 G allele has been linked to higher MPO mRNA and protein expression than the –463A allele in human and transgenic mouse monocyte–macrophages [11,12]. Elevated serum MPO is an indicator of heightened risk of CAD events [13], whereas individuals with inherited MPO deficiencies have reduced cardiovascular disease [14].

Apoptotic endothelial cells contribute to endothelial dysfunction and destabilization of atherosclerotic plaques and thrombosis, suggesting that endothelial cell apoptosis plays an important role in initiation and progression of atherosclerosis [15]. A wide variety of stimuli such as oxidative stress can induce apoptosis of endothelial cells and endothelial dysfunction, which may be regulated by different signal pathways [16]. Mitogen-activated protein kinases (MAPKs), including p38 MAPK, extracellular signal-regulated kinase 1/2 (ERK1/2), and c-Jun NH_2-terminal kinase (JNK), are a family of central signaling molecules that respond to numerous stimuli and are known to participate in cell survival and death decisions [17–19]. Among them, phosphorylation of ERK1/2 promotes cell survival, whereas activation of JNK and p38 MAPK induces apoptotic responses in endothelial cells. Evidences have been demonstrated that ROS can activate JNK/p38 MAPK, which triggers subsequent apoptosis programs such as activation of the caspase protease family in certain cells [20,21]. There are more than 10 caspase protease family members and they are thought to be downstream executors of apoptosis. Among them, caspase-3 has been considered to be a central component of the proteolytic cascade and to play a key role in apoptosis [22].

Vascular peroxidase 1 (VPO1) is a newly discovered member of the peroxidase family [23]. VPO1 is an isozyme of MPO. MPO exists only in neutrophils and monocyte–macrophages [24]. VPO1 is mainly expressed in vascular endothelial cells and smooth muscle cells, and it has structural characteristics and biological activity similar to those of MPO [23]. There is convincing evidence that MPO plays an important role in atherogenesis, as mentioned above; we therefore hypothesized that VPO1 may also be involved in the genesis and development of atherosclerosis.

Our specific aims were to explore the role of VPO1 in oxidized-LDL (ox-LDL)-induced apoptosis of endothelial cells. It has been well documented that the NADPH oxidase/ROS/p38 MAPK/caspase-3 pathway is involved in ox-LDL-induced endothelial cell apoptosis [18,25,26]. We therefore determined the relationship between VPO1 and this now-accepted dogma in mediating ox-LDL-induced endothelial cell apoptosis. The issue will help to

further clarify the biological role of VPO1 and provide some new perspectives on the prevention and treatment of cardiovascular diseases including atherosclerosis.

1. Materials and methods

1.1. Materials

Dulbecco's modified Eagle's medium (DMEM), penicillin, and streptomycin were obtained from Gibco BRL. Fetal bovine serum (FBS) was obtained from Sijiqing Biological Engineering Materials (Hangzhou, China). All primary antibodies except anti-VPO1 antibody were purchased from Santa Cruz Biotechnology (Santa Cruz, CA, USA). Apocynin, diphenyliodonium (DPI), SB203580, and the caspase-3 activity assay kits were purchased from Sigma (St. Louis, MO, USA); acetyl-DEVD-CHO was purchased from Calbiochem (San Diego, CA, USA); fluorescein isothiocyanate (FITC)–annexin V and propidium iodide (PI) were obtained from Jingmei Biotech (Shenzheng, China); Hoechst 33342 and the fluorescent ROS detection kit were purchased from Beytime Biotechnology (Jiangsu, China); all other biochemicals used were of the highest purity available.

1.2. Cell culture and transfection

Human umbilical vein endothelial cells (HUVECs) were originally purchased from the ATCC. HUVECs were cultured according to standard procedure as described previously [13]. Cells were seeded at a density of 3×10^5 per 100-mm dish in DMEM supplemented with 20 mM Hepes and 20% FBS. The cultures were kept at 37 °C with a gas mixture of 5% CO_2/95% air. The medium was supplemented with 5 U/ml heparin, 100 IU/ml penicillin, and 100 μg/ml streptomycin. Endothelial cells of the fourth to sixth passages in the actively growing condition were used for experiments.

High-performance purity-grade (90% purity) small-hairpin RNAs (shRNAs) against VPO1 (VPO1-shRNA) were obtained from Genechem (Shanghai, China). shRNA with a nonsilencing oligonucleotide sequence that does not have any known homology to mammalian genes was used as a negative control (control-shRNA). HUVECs were plated in six-well plates and grown in DMEM containing 10% FBS. One day after seeding, the cells were transfected with 100 pmol of control-shRNA or 100 pmol of VPO1-shRNA using Lipofectamine NAiFect transfection reagent (Qiagen) according to the manufacturer's instructions. Four hours after transfection, the cells were washed with Hanks' buffered saline solution, then DMEM containing 10% FBS was added. Two days later the cells were trypsinized and split into 100-mm petri dishes. G418 (400 μg/ml; Gibco BRL) was added to the culture and changed every 1 or 2 days. When the first resistant clones were detected, the concentration of G418 was decreased to 200 μg/ml. Individual clones were pipetted off, transferred, and grown into clonal lines in medium containing G418 (200 μg/ml). The infection efficiency was evaluated by green fluorescent protein (GFP) expression using fluorescence microscopy and by VPO1 expression using Western blotting analysis.

Small interfering RNA (siRNA) against NADPH oxidase $gp91^{phox}$ subunit (Genechem) was generated against the following human NADPH oxidase $gp91^{phox}$ mRNA sequences: sense, 5′-CGUCUUCCU-CUUUGUCUGGdTdT-3′; antisense, 5′-CCAGACAAAGAGGAA-GACGdTdT-3′. As described previously [17], HUVECs grown to 60 to 70% confluence were transfected with Gene Silencer transfection reagent according to the manufacturer's instructions, plus $gp91^{phox}$ siRNA or control nontargeting siRNA in FBS-free DMEM. Three hours after transfection, fresh DMEM supplemented with 5% FBS and without endothelial growth supplement was added, and the cells were cultured in the presence or absence of ox-LDL for an additional 24 h. The infection efficiency was evaluated by $gp91^{phox}$ expression using Western blotting analysis.

1.3. Experimental protocol

To investigate the effects of ox-LDL on endothelial cell apoptosis and VPO1 expression, the cells were treated with ox-LDL (100 μg/ml) for 12, 24, or 48 h or ox-LDL (50, 100, or 200 μg/ml) for 24 h. To further examine the role of the NADPH oxidase/ROS/VPO1/HOCl/p38 MAPK/caspase-3 pathway in ox-LDL-induced endothelial cell apoptosis, two series experiments were performed. First, cells were pretreated with 600 μM apocynin (the NADPH oxidase inhibitor), 10 μM DPI (the NADPH oxidase inhibitor), 1 μM SB203580 (the specific p38 MAPK inhibitor), or 100 μM DEVD-CHO (the specific caspase-3 inhibitor) for 1 h, or successfully transfected with VPO1-shRNA or $gp91^{phox}$ siRNA, and then exposed to ox-LDL (100 μg/ml) for 24 h. The protein expression of NADPH oxidase $gp91^{phox}$ subunit, VPO1, p38 MAPK, and β-actin; caspase-3 activity; and apoptosis were then determined. Second, wild-type cells or cells successfully transfected with VPO1-shRNA/$gp91^{phox}$ siRNA were harvested and suspended in 10 mM phosphate buffer (pH 7.4, 37 °C) containing 140 mM sodium chloride, 10 mM potassium chloride, 0.5 mM magnesium chloride, 1 mM calcium chloride, 1 mg/ml glucose, and 5 mM taurine. The cells were pretreated with 600 μM apocynin or 10 μM DPI for 1 h, then exposed to ox-LDL (100 μg/ml) for 30 min, and intracellular ROS or HOCl levels in the supernatant were determined.

1.4. Preparation of LDL and LDL oxidation by copper

Native LDL was isolated from pooled plasma of healthy donors through sequential density gradient ultracentrifugation in sodium bromide density solutions in the density range of 1.019–1.063 kg/L as previously described [25]. Then isolated LDL was dialyzed under nitrogen for 24 h at 4 °C against phosphate-buffered saline (PBS; 5 mM phosphate buffer and 125 mM NaCl, pH 7.4). LDL was oxidized by dialysis for 24 h at 37 °C against 10 μM $CuSO_4$ in PBS, as previously described in detail, and then the oxidized LDL was dialyzed for 24 h at 4 °C against PBS containing 0.3 mM EDTA. Protein concentration was measured by Lowry's method. The levels of thiobarbituric acid-reactive substances (TBARS), reflecting the extent of LDL oxidation, were measured by previously described methods [25]. The levels of TBARS were 6.15±0.88 and 25.12±6.78 μM/g protein for LDL and ox-LDL, respectively.

1.5. Apoptosis determination

1.5.1. Annexin V–PI double-staining assay—Cells were collected and washed with PBS two times and then were resuspended in 250 μl binding buffer. FITC–annexin V (5 μl) and PI (10 μl, 20 μg/ml) were diluted per 100 μl cell suspension. The cells were incubated at room temperature for 15 min. After 400 μl PBS was added to the mixture, the samples were analyzed by flow cytometry (Becton–Dickinson).

1.5.2. Hoechst 33342 staining assay—Cells were cultured in 24-well plates and treated with Hoechst 33342 (100 μg/ml) for 10 min at 37 °C in the dark. Hoechst-stained nuclei were observed using a fluorescence microscope (Olympus, Japan) at 521 nm emission wavelength. A total of 200 cells from five random high-power fields were counted. The percentage of apoptosis was expressed as the ratio of apoptotic cells to total cells.

1.6. Measurement of intracellular ROS

Changes in intracellular ROS levels were determined by measuring the oxidative conversion of cell-permeative 2′,7′-dichlorofluorescein diacetate (H_2DCF) to fluorescent dichlorofluorescein (DCF) in a fluorescence spectrophotometer (F4000; Hitachi, Japan). H_2DCF was added at a final concentration of 10 μM and incubated for 20 min at 37 °C. The fluorescence was monitored using a fluorescence microscope equipped with an FITC filter

and the average intensity values were measured at 200× magnification in five randomly chosen fields for each of nine replicates from four independent experiments.

1.7. Hypochlorous acid assay

HOCl can be trapped with taurine to form a stable chloramine. Chloramines are detected by using iodide to catalyze the oxidation of 3,3′,5,5′-tetramethylbenzidine (TMB) to form strongly absorbing products. We therefore used a TMB assay to determine HOCl production [27]. In brief, the cells were harvested and suspended in 10 mM phosphate buffer (pH 7.4, 37 °C) containing 140 mM sodium chloride, 10 mM potassium chloride, 0.5 mM magnesium chloride, 1 mM calcium chloride, 1 mg/ml glucose, and 5 mM taurine. Reactions were carried out in 1.5-ml Eppendorf centrifuge tubes. The tubes were rotated gently every 5 min to ensure that the cells were kept in suspension and fully aerated. Reactions were stopped by the addition of 20 μg/ml catalase and placement of tubes in melting ice for at least 10 min. The cells were then pelleted by centrifugation (5 min at 14,000 *g*). The supernatant (200 μl) was rapidly and completely mixed with 50 μl of TMB, 100 μM sodium iodide, and 10% dimethylformamide in 400 mM acetate buffer. After 5 min the absorbance at 650 nm was recorded and related to the standard curve to determine the concentration of taurine chloramine. HOCl production was calculated by the standard curve of the TMB method.

1.8. Measurement of caspase-3 activity

The activity of caspase-3-like protease in the lysate was measured using a colorimetric caspase-3 assay kit according to the manufacturer's protocol. In brief, cytosolic protein (100 μg) was mixed with caspase-3-specific substrate acetyl-Asp-Glu-Val-Asp-*p*-nitroanilide (final concentration, 200 μM) and incubated at 37 °C for 90 min. The absorbance was read at 405 nm. To confirm that substrate cleavage was due to caspase activity, extracts were incubated in the presence of the caspase-3-specific inhibitor acetyl-DEVD-CHO (final concentration, 20 μM) at 37 °C, before the addition of substrate. The value (in arbitrary absorbance units) of the absorbance signal of the inhibited sample was subtracted from that of the noninhibited sample.

1.9. Anti-VPO1 antibody

A region of the VPO1 peroxidase domain with highly predicted antigenicity was chosen using DNA Star software (Madison, WI, USA). The peptide (corresponding to residues 1197–1211) was synthesized, purified by reverse-phase high-performance liquid chromatography, and conjugated with keyhole limpet hemocyanin from Sigma–Genosys (The Woodlands, TX, USA). Anti-VPO1 antibody was raised in rabbit against the conjugated peptide (Sigma–Genosys). Antibody was purified using protein G–agarose beads according to standard procedures. The specificity of the antiserum was determined by Western blotting as in our previous study [23].

1.10. Real-time RT-PCR analysis

The mRNA expression of VPO1 in HUVECs was analyzed using the ABI 7300 real-time PCR system (Foster City, CA, USA). The specific primer pairs were human, 5′-AGCCAGCCATCACCTGGAAC-3′ (forward) and 5′-TTCCGGGCCACACACTCATA-3′ (backward). Reverse-transcription reaction was performed with 1 μg total RNA isolated from the cells of each group. For PCR amplification, cDNAs were amplified using the SYBR green real-time PCR master mix (TaKaRa) and 0.4 μM each primer pair. Amplification was carried out starting with an initial step for 30 s at 94 °C, followed by 40 cycles of the amplification step (94 °C for 30 s,60 °C for 60 s, and 72 °C for 1 min) for VPO1 or GAPDH. All amplification reactions for each sample were carried out in triplicate

and the averages of the threshold cycles were used to interpolate curves using 7300 System SDS software. Results were expressed as the ratio of VPO1 to GAPDH mRNA, and the VPO1 expression level in the control group was regarded as 100%.

1.11. Western blot analysis

Cells were lysed for 30 min at 4 °C in a lysis buffer. Total cell protein concentration was determined using the bicinchoninic acid reagent. Total protein (50 to 100 μg) was resolved by SDS–polyacrylamide gel electrophoresis, transferred to a nitrocellulose membrane, and subjected to immunoblot analysis. The primary antibodies for VPO1 (1:2000), p38 MAPK (1:1000), NADPH oxidase $gp91^{phox}$ subunit (1:2000), or β-actin (1:1000) and horseradish peroxidase-conjugated secondary antibody (Santa Cruz Biotechnology) were used. The bands were visualized using enhanced chemiluminescence reagents and analyzed with a gel documentation system (Bio-Rad Gel Doc1000 and Multi-Analyst version 1.1). All results were representative of at least three independent experiments.

1.12. Statistical analysis

Results are expressed as means±SEM. Data were analyzed by ANOVA followed by the Newman–Student–Keuls test for multiple comparisons. The significance level was chosen as $P<0.05$.

2. Results

2.1. Effects of ox-LDL on apoptosis and VPO1 expression in HUVECs

In keeping with previous study [26], treatment of HUVECs with ox-LDL (0, 50, 100, or 200 μg/ml) for 0, 12, 24, and 48 h induced apoptosis in a concentration- and time-dependent manner (Figs. 1A and B, respectively). Hoechst 33342 staining assay showed that treatment with ox-LDL significantly increased the ratio of cells with a profile of cell shrinkage, chromatin condensation, and fragmented fluorescent nuclei. Annexin V–PI staining assay with flow cytometry also showed that treatment with ox-LDL significantly increased the ratio of apoptotic cells. Importantly, we found that ox-LDL time- and concentration-dependently up-regulated VPO1 expression (both mRNA and protein) (Figs. 2A–D).

2.2. Role of VPO1 in ox-LDL-induced apoptosis in HUVECs

To investigate the role of VPO1 in mediation of ox-LDL-induced apoptosis of endothelial cells, the strategy of VPO1 RNA interference was applied. As shown in Fig. 2E, more than 90% cells transfected with VPO1-shRNA showed GFP expression. Transfection of HUVECs with VPO1-shRNA successfully knocked down the VPO1 protein expression (Fig. 2F). In contrast, control-shRNA, nontargeting to any known cDNA, did not affect the VPO1 expression.

Importantly, annexin V–PI staining assay with flow cytometry showed that shRNA targeting VPO1 significantly inhibited ox-LDL-induced apoptosis in HUVECs (Fig. 3A). The increased caspase-3 activity induced by ox-LDL, a marker of apoptosis, was also inhibited by VPO1 shRNA in HUVECs (Fig. 3B). VPO1 shRNA alone had no effect on cell apoptosis or caspase-3 activity.

2.3. Role of NADPH oxidase/p38 MAPK/caspase-3 pathway in ox-LDL-induced apoptosis in HUVECs

In line with previous studies [18,26,28], pretreatment with the NADPH oxidase inhibitors (apocynin and DPI), NADPH oxidase gene-silencing using $gp91^{phox}$ siRNA transfection, the specific p38MAPK inhibitor SB203580, or the specific caspase-3 inhibitor DEVD-CHO

significantly inhibited ox-LDL-induced endothelial cell apoptosis and the increased caspase-3 activity (Figs. 3A, B, C, and D). Apocynin (Figs. 3A and B), DPI, $gp91^{phox}$ siRNA (Figs. 3C and D), SB203580, or DEVD-CHO (data not shown) alone had no effect on cell apoptosis or caspase-3 activity.

2.4. Relationship between VPO1/HOCl and NADPH oxidase/ROS/p38 MAPK pathway in ox-LDL-induced apoptosis in HUVECs

VPO1 expressed in live cells can use H_2O_2 generated from coexpressed NADPH oxidases directly to produce HOCl and its chlorinating species to catalyze peroxidative reactions [23]. To determine the relationship between the VPO1/HOCl and the NADPH oxidase/ROS/p38 MAPK pathways in mediating ox-LDL-induced apoptosis in HUVECs, we used the specific inhibitors apocynin, DPI, SB203580, and DEVD-CHO and the strategy of shRNA targeting to VPO1 and siRNA against NADPH oxidase subunit $gp91^{phox}$. Apocynin, DPI, $gp91^{phox}$ siRNA, and VPO1 shRNA significantly inhibited ox-LDL-induced intracellular ROS and HOCl generation (Figs. A, B, C, and 4D and Supplementary Fig. S1). Importantly, apocynin, DPI, $gp91^{phox}$ siRNA, and VPO1 shRNA also down-regulated the protein expression of VPO1 and NADPH oxidase $gp91^{phox}$ subunit and decreased the phosphorylation of p38 MAPK in the presence of ox-LDL (Figs. 5A, B, C, and D). Apocynin, DPI, $gp91^{phox}$ siRNA, or VPO1 shRNA alone had no effect on intracellular ROS and HOCl generation (Figs. 4A, B, C, and D). Apocynin or DPI alone had no effect on the protein expression of VPO1 or NADPH oxidase $gp91^{phox}$ subunit or the phosphorylation of p38 MAPK (Figs. 5A, B, C, and D). VPO1 shRNA alone had no effect on the protein expression of NADPH oxidase $gp91^{phox}$ subunit, but significantly down-regulated the basal expression of VPO1 and phosphorylated p38MAPK (Figs. 5A, B, C, and D). $gp91^{phox}$ siRNA alone significantly down-regulated the basal expression of $gp91^{phox}$ and VPO1 as well as phosphorylated p38MAPK (Figs. 5A, B, C, and D). It is of note that SB203580 or DEVD-CHO had no effect on intracellular ROS or HOCl generation or the protein expression of VPO1 or NADPH oxidase $gp91^{phox}$ subunit (data not shown).

3. Discussion

This study revealed that ox-LDL induced endothelial cell apoptosis and the expression of VPO1 in endothelial cells in a concentration-and time-dependent manner concomitant with increased intracellular ROS and HOCl generation and the up-regulated protein expression of NADPH oxidase $gp91^{phox}$ subunit and phosphorylation of p38 MAPK. All these effects of ox-LDL were inhibited by VPO1 and NADPH oxidase $gp91^{phox}$ subunit gene silencing or by pretreatment with apocynin and DPI (the NADPH oxidase inhibitors). The p38 MAPK inhibitor SB203580, or the caspase-3 inhibitor DEVD-CHO, significantly inhibited ox-LDL-induced endothelial cell apoptosis, but had no effect on intracellular ROS or HOCl generation or the expression of NADPH oxidase $gp91^{phox}$ subunit and VPO1. Collectively, these findings suggest for the first time that VPO1 plays a critical role in ox-LDL-induced endothelial cell apoptosis and that there is a positive feedback loop between VPO1/HOCl and the now-accepted dogma that the NADPH oxidase/ROS/p38 MAPK/caspase-3 pathway is involved in ox-LDL-induced endothelial cell apoptosis.

Thrombosis underlies most acute complications of atherosclerosis, notably acute coronary syndromes (ACS) [29]. Coronary thrombosis may arise not only from a fracture in the plaque's protective fibrous cap, but also from superficial erosion of the luminal endothelium without a rupture extending into the lipid core [30]. In approximately one-quarter of cases of sudden cardiac death, fatal thrombosis in the coronary arteries results from superficial erosion of coronary fibrous plaques morphologically recognized as "stable plaques" [31,32]. This mechanism of plaque disruption appears more common in women and smokers. Disordered metabolism of interstitial collagen probably sets the stage for fibrous cap rupture

in lipid-rich atheroma [31]. However, the molecular mechanisms of endothelial erosion in atherosclerotic plaques are uncertain. Several lines of evidence support the presence of apoptosis of endothelial cells (ECs) in atheroma as well as increased circulating apoptotic ECs in patients with ACS, suggesting that EC death atop the atherosclerotic arterial intima participates in endothelial desquamation and subsequent thrombosis [33].

Our previous study demonstrated that VPO1 expressed in live cells could use H_2O_2 generated from coexpressed NADPH oxidases directly to produce HOCl and its chlorinating species to catalyze peroxidative reactions [23]. As the NADPH oxidases are normally expressed in the same vascular cells where VPO1 is expressed, one can speculate that VPO1 is likely to play an important role in the vascular system. Such a role in the vascular system could involve defense against microbes that enter or colonize the vasculature; an analogous role is seen with lactoperoxidase in the salivary gland and bronchi, where it has an antimicrobial effect in the alimentary and upper airway systems [34]. Alternatively, VPO1 may carry out peroxidative reactions in the vascular system that have been previously attributed exclusively to MPO, and these might participate in the development of atherosclerosis. We demonstrated here for the first time that VPO1 gene silencing inhibited ox-LDL-induced endothelial cell apoptosis. Our study provides a potential mechanistic link for VPO1 to increase endothelial cell apoptosis in atherosclerosis.

The exact mechanism by which VPO1 influences cell apoptosis is unknown. In our previous studies [23], we have demonstrated that VPO1 can catalyze a reaction between hydrogen peroxide and chloride to generate potent oxidants including HOCl, which is similar to MPO. Studies show that HOCl can induce cell death by decreasing cellular ATP levels or modifying cell-surface proteins [35,36]. Recently, it has also been demonstrated that HOCl causes apoptosis and growth arrest in human ECs [37]. This study shows that sublethal concentrations of HOCl rapidly provoke apoptotic EC death, probably caused by Bcl-2 degradation and cytochrome *c* release from mitochondria. The precise mechanisms of HOCl-induced Bcl-2 loss remain uncertain at present. It has been shown that intracellular GSH depletion caused by buthionine sulfoximine induces degradation of the Bcl-2 protein and promotes apoptosis in cholangiocytes [38]. Otherwise, HOCl rapidly decreases the intracellular GSH levels in human ECs, suggesting that GSH depletion by HOCl might play a key role in the degradation of Bcl-2 protein in ECs [39]. Xue et al. have shown that locally generated ROS can directly destroy native Bcl-2 protein by a protease-independent mechanism [40]. Thus, Bcl-2 may be a direct or indirect intracellular target of HOCl, triggering the activation of the apoptotic cascade in human ECs. A previous study has also documented that chlorotyrosine, the oxidative product of HOCl, promotes endothelial cell apoptosis by activating the NADPH/ROS/p38 MAPK signal pathway [39,41]. And as one of heme-containing peroxidase enzymes, VPO1 participates in H_2O_2 metabolism, leading to production of HOCl and probably activating the NADPH/ROS/p38 MAPK signal pathway.

NADPH oxidase is an inducible electron transport system that transfers reducing equivalents from NADPH to molecular oxygen via flavins, resulting in $O_2^{\bullet -}$ generation [42]. A previous study has shown that NADPH oxidase is present in neutrophils [43]. Recent studies indicate that NADPH oxidase is also the major origin of ROS in some nonphagocytic cells, such as endothelial cells and smooth muscle cells [44,45]. It has been reported that the activity of NADPH oxidase is increased by up-regulation of gene expression and/or posttranscriptional expression at the protein level, and the enzyme-dependent oxidative stress is thought to play a pivotal role in endothelial dysfunction of some cardiovascular diseases [46,47]. Ox-LDL, the main component of serum lipids, is a crucial risk factor for atherosclerosis and endothelial dysfunction [48]. Numerous studies have suggested that NADPH oxidase plays an important role in ox-LDL-induced oxidative stress, in that ox-LDL can induce ROS generation by increasing NADPH oxidase activity in the endothelium [49,50]. More

significantly, the increase in ROS is both required and sufficient to generate the physiological changes that accompany the generation of an atherosclerotic endothelium. There is evidence to suggest that the proliferation and migration of the endothelium induced by ox-LDL are mediated by NADPH oxidase [51]. Pretreatment with the NADPH oxidase inhibitor, DPI, attenuated the effects of ox-LDL. In this study, we confirmed the previous studies showing that ox-LDL significantly up-regulated the expression of NADPH oxidase and subsequently enhanced the production of intracellular ROS in HUVECs, an effect that was attenuated by the NADPH oxidase inhibitors apocynin and DPI, or by NADPH oxidase $gp91^{phox}$ subunit, or by VPO1 gene silencing.

It has been reported that activation of p38 MAPK or its upstream kinases in cells induces apoptosis, and blocking the activation of p38 MAPK protects against apoptosis in several cell lines [26,52]. In this study, we found that ox-LDL could induce activation of p38 MAPK, congruent with the increase in cell apoptosis. In addition, treatment with a p38-MAPK-specific inhibitor could effectively abolish ox-LDL-induced cell apoptosis. Therefore, these results suggest that the activation of p38 MAPK contributes to ox-LDL-induced apoptotic death of endothelial cells.

Caspase family proteases can activate themselves in vitro, and some can activate other family members, which in turn cleave various substrate proteins that account for many of the biochemical and morphological changes that occur during apoptosis. Among them, caspase-3 has been considered a central component of the proteolytic cascade during apoptosis [22]. We examined the substrate specificity of proteolytic activity and identified a significantly increased caspase-3 activity in the extracts from ox-LDL-treated endothelial cells. The apoptosis induced by ox-LDL could be inhibited by DEVD-CHO, the caspase-3-specific inhibitor. Our current data further confirmed that caspase-3 might be a predominant target involved in ox-LDL-induced apoptosis in endothelial cells. Cross talk between p38 MAPK and caspase signaling pathways has been previously reported in endothelial cells [18,53]. However, it is unclear as to whether p38 MAPK is upstream of caspases or vice versa. We showed that the increased p38 MAPK phosphorylation induced by ox-LDL could be effectively suppressed by the NADPH oxidase inhibitors apocynin and DPI, or by NADPH oxidase $gp91^{phox}$ subunit, or by VPO1 gene silencing. Moreover, we found that the p38-MAPK-specific inhibitor was capable of inhibiting the caspase-3 activation in endothelial cells treated with ox-LDL. These findings implied that ROS induced by ox-LDL may be involved in p38 MAPK phosphorylation, which in turn triggers caspase-3 activation in human endothelial cells.

In summary, our study is the first report documenting that VPO1, a newly identified heme-containing peroxidase, induces endothelial cell apoptosis via elevation of intracellular ROS and HOCl, for which there is a positive feedback loop between VPO1 and NADPH oxidase and which in turn activates the p38 MAPK/caspase-3-dependent signaling pathway. The proposed pathway of VPO1 mediation of ox-LDL-induced endothelial cell apoptosis is summarized in Fig. 6. We believe that VPO1 may be a potential therapeutic target in cardiovascular diseases including atherogenesis. It is of note that in our setting the detection of HOCl in the supernatant could be due to the release of VPO1 although we also detected intracellular production of HOCl as shown in the online supplementary data. Therefore, the significance of VPO1 as a potential intracellular secretory protein deserves to be further investigated.

Supplementary Material

Refer to Web version on PubMed Central for supplementary material.

Acknowledgments

This study was supported by grants from the Natural Science Foundation of China (Nos. 30871052 and 30971194) and the Graduate Degree Thesis Innovation Foundation of Central South University (Nos. 2008yb029 and 2960–71131100011) and U.S. National Institutes of Health (NIH/NHLBI) Grant R01 HL086836 (to G. Cheng).

References

1. Malle E, Waeg G, Schreiber R, Gröne EF, Sattler W, Gröne HJ. Immunohistochemical evidence for the myeloperoxidase/H_2O_2/halide system in human atherosclerotic lesions. Eur J Biochem. 2000; 267:4495–4503. [PubMed: 10880973]
2. Podrez EA, Abu-Soud HM, Hazen SL. Myeloperoxidase-generated oxidants and atherosclerosis. Free Radic Biol Med. 2000; 28:1717–1725. [PubMed: 10946213]
3. Stocker R, Huang A, Jeranian E, Hou JY, Wu TT, Thomas SR, Keaney JF Jr. Hypochlorous acid impairs endothelium-derived nitric oxide bioactivity through a superoxide-dependent mechanism. Arterioscler Thromb Vasc Biol. 2004; 24:2028–2033. [PubMed: 15331437]
4. Woods AA, Linton SM, Davies MJ. Detection of HOCl-mediated protein oxidation products in the extracellular matrix of human atherosclerotic plaques. Biochem J. 2003; 370:729–735. [PubMed: 12456264]
5. Malle E, Marsche G, Arnhold J, Davies MJ. Modification of low-density lipoprotein by myeloperoxidase-derived oxidants and reagent hypochlorous acid. Biochim Biophys Acta. 2006; 1761:392–415. [PubMed: 16698314]
6. Hazen SL, Hsu FF, Gaut JP, Crowley JR, Heinecke JW. Modification of proteins and lipids by myeloperoxidase. Methods Enzymol. 1999; 300:88–105. [PubMed: 9919513]
7. Nicholls SJ, Hazen SL. Myeloperoxidase, modified lipoproteins, and atherogenesis. J Lipid Res. 2009; 50:346–351.
8. Shao B, Oda MN, Bergt C, Fu X, Green PS, Brot N, Oram JF, Heinecke JW. Myeloperoxidase impairs ABCA1-dependent cholesterol efflux through methionine oxidation and site-specific tyrosine chlorination of apolipoprotein A-I. J Biol Chem. 2006; 281:9001–9004. [PubMed: 16497665]
9. Kumar AP, Ryan C, Cordy V, Reynolds WF. Inducible nitric oxide synthase expression is inhibited by myeloperoxidase. Nitric Oxide. 2005; 13:42–53. [PubMed: 15893945]
10. Asselbergs FW, Reynolds WF, Cohen-Tervaert JW, Jessurun GA, Tio RA. Myeloperoxidase polymorphism related to cardiovascular events in coronary artery disease. Am J Med. 2004; 116:429–430. [PubMed: 15006595]
11. Nikpoor B, Turecki G, Fournier C, Théroux P, Rouleau GA. A functional myeloperoxidase polymorphic variant is associated with coronary artery disease in French-Canadians. Am Heart J. 2001; 142:336–339. [PubMed: 11479475]
12. Castellani LW, Chang JJ, Wang X, Lusis AJ, Reynolds WF. Transgenic mice express human MPO –463 G/A alleles at atherosclerotic lesions, developing hyperlipidemia and obesity in –463 G males. J Lipid Res. 2006; 47:1366–1377. [PubMed: 16639078]
13. Zhang R, Brennan ML, Fu X, Aviles RJ, Pearce GL, Penn MS, Topol EJ, Sprecher DL, Hazen SL. Association between myeloperoxidase levels and risk of coronary artery disease. JAMA. 2001; 286:2136–2142. [PubMed: 11694155]
14. Kutter D, Devaquet P, Vanderstocken G, Paulus JM, Marchal V, Gothot A. Consequences of total and subtotal myeloperoxidase deficiency: risk or benefit ? Acta Haematol. 2000; 104:10–15. [PubMed: 11111115]
15. Xu F, Sun Y, Chen Y, Sun Y, Li R, Liu C, Zhang C, Wang R, Zhang Y. Endothelial cell apoptosis is responsible for the formation of coronary thrombotic atherosclerotic plaques. Tohoku J Exp Med. 2009; 218:25–33. [PubMed: 19398870]
16. Davignon J, Ganz P. Role of endothelial dysfunction in atherosclerosis. Circulation. 2004; 109:27–32.
17. Dandapat A, Hu C, Sun L, Mehta JL. Small concentrations of oxLDL induce capillary tube formation from endothelial cells via LOX-1-dependent redox-sensitive pathway. Arterioscler Thromb Vasc Biol. 2007; 27:2435–2442. [PubMed: 17717293]

18. Takahashi M, Okazaki H, Ogata Y, Takeuchi K, Ikeda U, Shimada K. Lysophosphatidylcholine induces apoptosis in human endothelial cells through a p38-mitogen-activated protein kinase-dependent mechanism. Atherosclerosis. 2002; 161:387–394. [PubMed: 11888522]
19. Davis RJ. Signal transduction by the JNK group of MAP kinases. Cell. 2000; 103:239–252. [PubMed: 11057897]
20. N'Guessan PD, Schmeck B, Ayim A, Hocke AC, Brell B, Hammerschmidt S, Rosseau S, Suttorp N, Hippenstiel S. Streptococcus pneumoniae R6x induced p38 MAPK and JNK-mediated caspase-dependent apoptosis in human endothelial cells. Thromb Haemostasis. 2005; 94:295–303. [PubMed: 16113818]
21. Osone S, Hosoi H, Kuwahara Y, Matsumoto Y, Iehara T, Sugimoto T. Fenretinide induces sustained-activation of JNK/p38 MAPK and apoptosis in a reactive oxygen species-dependent manner in neuroblastoma cells. Int J Cancer. 2004; 112:219–224. [PubMed: 15352033]
22. Porter AG, Janicke RU. Emerging roles of caspase-3 in apoptosis. Cell Death. 1999; 6:99–104.
23. Cheng G, Salerno JC, Cao Z, Pagano PJ, Lambeth JD. Identification and characterization of VPO1, a new animal heme-containing peroxidase. Free Radic Biol Med. 2008; 45:1682–1694. [PubMed: 18929642]
24. Malle E, Furtmüller PG, Sattler W, Obinger C. Myeloperoxidase: a target for new drug development? Br J Pharmacol. 2007; 152:838–854. [PubMed: 17592500]
25. Bai YP, Hu CP, Chen MF, Xu KP, Tang GS, Shi RZ, Li YJ, Zhang GG. Inhibitory effect of reinioside C on monocyte–endothelial cell adhesion induced by oxidized low-density lipoprotein via inhibiting NADPH oxidase/ROS/NF-κB pathway. Naunyn-Schmiedeberg's Arch Pharmacol. 2009; 380:399–406. [PubMed: 19730822]
26. Nihei S, Yamashita K, Tasaki H, Ozumi K, Nakashima Y. Oxidized low-density lipoprotein-induced apoptosis is attenuated by insulin-activated phosphatidylinositol 3-kinase/Akt through p38 mitogen-activated protein kinase. Clin Exp Pharmacol Physiol. 2005; 32:224–229. [PubMed: 15743407]
27. Dypbukt JM, Bishop C, Brooks WM, Thong B, Eriksson H, Kettle AJ. A sensitive and selective assay for chloramine production by myeloperoxidase. Free Radic Biol Med. 2005; 39:1468–1477. [PubMed: 16274882]
28. Chen XP, Xun KL, Wu Q, Zhang TT, Shi JS, Du GH. Oxidized low density lipoprotein receptor-1 mediates oxidized low density lipoprotein-induced apoptosis in human umbilical vein endothelial cells: role of reactive oxygen species. Vasc Pharmacol. 2007; 47:1–9.
29. Libby P. Molecular bases of the acute coronary syndromes. Circulation. 1995; 91:2844–2850. [PubMed: 7758192]
30. Libby P. Current concepts of the pathogenesis of the acute coronary syndromes. Circulation. 2001; 104:365–372. [PubMed: 11457759]
31. Farb A, Burke AP, Tang AL, Liang TY, Mannan P, Smialek J, Virmani R. Coronary plaque erosion without rupture into a lipid core: a frequent cause of coronary thrombosis in sudden coronary death. Circulation. 1996; 93:1354–1363. [PubMed: 8641024]
32. Arbustini E, Dal Bello B, Morbini P, Burke AP, Bocciarelli M, Specchia G, Virmani R. Plaque erosion is a major substrate for coronary thrombosis in acute myocardial infarction. Heart. 1999; 82:269–272. [PubMed: 10455073]
33. Mallat Z, Tedgui A. Current perspective on the roleof apoptosis in atherothrombotic disease. Circ Res. 2001; 88:998–1003. [PubMed: 11375268]
34. Geiszt M, Witta J, Baffi J, Lekstrom K, Leto TL. Dual oxidases represent novel hydrogen peroxide sources supporting mucosal surface host defense. FASEB J. 2003; 17:1502–1504. [PubMed: 12824283]
35. Schraufstatter IU, Browne K, Harris A, Hyslop PA, Jackson JH, Quehenberger O, Cochrane CG. Mechanisms of hypochlorite injury of target cells. J Clin Invest. 1990; 85:554–562. [PubMed: 2153710]
36. Vissers MC, Carr AC, Chapman AL. Comparison of human red cell lysis by hypochlorous and hypobromous acids: insights into the mechanism of lysis. Biochem J. 1998; 330:131–138. [PubMed: 9461501]

37. Vissers MC, Pullar JM, Hampton MB. Hypochlorous acid causes caspase activation and apoptosis or growth arrest in human endothelial cells. Biochem J. 1999; 344:443–449. [PubMed: 10567227]
38. Celli A, Que FG, Gores GJ, LaRusso NF. Glutathione depletion is associated with decreased Bcl-2 expression and increased apoptosis in cholangiocytes. Am J Physiol. 1998; 275:749–757.
39. Sugiyama S, Kugiyama K, Aikawa M, Nakamura S, Ogawa H, Libby P. Hypochlorous acid, a macrophage product, induces endothelial apoptosis and tissue factor expression: involvement of myeloperoxidase-mediated oxidant in plaque erosion and thrombogenesis. Arterioscler Thromb Vasc Biol. 2004; 24:1309–1314. [PubMed: 15142860]
40. Xue LY, Chiu SM, Oleinick NL. Photochemical destruction of the Bcl-2 oncoprotein during photodynamic therapy with the phthalocyanine photosensitizer Pc 4. Oncogene. 2001; 20:3420–3427. [PubMed: 11423992]
41. Vicca S, Massy ZA, Hennequin C, Rihane D, Drüeke TB, Lacour B. Apoptotic pathways involved in U937 cells exposed to LDL oxidized by hypochlorous acid. Free Radic Biol Med. 2003; 35:603–615. [PubMed: 12957653]
42. Dworakowski R, Anilkumar N, Zhang M, Shah AM. Redox signalling involving NADPH oxidase-derived reactive oxygen species. Biochem Soc Trans. 2006; 34:960–964. [PubMed: 17052237]
43. Cox JA, Jeng AY, Sharkey NA, Blumberg PM, Tauber AI. Activation of the human neutrophil nicotinamide adenine dinucleotide phosphate (NADPH)-oxidase by protein kinase C. J Clin Invest. 1985; 76:1932–1938. [PubMed: 2997297]
44. Paravicini TM, Touyz RM. NADPH oxidases, reactive oxygen species, and hypertension: clinical implications and therapeutic possibilities. Diabetes Care. 2008; 2:170–180.
45. Frey RS, Ushio-Fukai M, Malik AB. NADPH oxidase-dependent signaling in endothelial cells: role in physiology and pathophysiology. Antioxid Redox Signaling. 2009; 11:791–810.
46. Brandes RP. Vascular functions of NADPH oxidases. Hypertension. 2010; 56:17–21. [PubMed: 20479337]
47. Muller G, Morawietz H. Nitric oxide, NAD(P)H oxidase, and atherosclerosis. Antioxid Redox Signaling. 2009; 11:1711–1731.
48. Kita T, Kume N, Minami M, Hayashida K, Murayama T, Sano H, Moriwaki H, Kataoka H, Nishi E, Horiuchi H, Arai H, Yokode M. Role of oxidized LDL in atherosclerosis. Ann N Y Acad Sci. 2001; 947:199–205. [PubMed: 11795267]
49. Stielow C, Catar RA, Muller G, Wingler K, Scheurer P, Schmidt HH, Morawietz H. Novel Nox inhibitor of oxLDL-induced reactive oxygen species formation in human endothelial cells. Biochem Biophys Res Commun. 2006; 344:200–205. [PubMed: 16603125]
50. Jia SJ, Jiang DJ, Hu CP, Zhang XH, Deng HW, Li YJ. Lysophosphatidylcho-line-induced elevation of asymmetric dimethylarginine level by the NADPH oxidase pathway in endothelial cells. Vasc Pharmacol. 2006; 44:143–148.
51. Abid MR, Kachra Z, Spokes KC, Aird WC. NADPH oxidase activity is required for endothelial cell proliferation and migration. FEBS Lett. 2000; 486:252–256. [PubMed: 11119713]
52. Jiang H, Liang C, Liu X, Jiang Q, He Z, Wu J, Pan X, Ren Y, Fan M, Li M, Wu Z. Palmitic acid promotes endothelial progenitor cells apoptosis via p38 and JNK mitogen-activated protein kinase pathways. Atherosclerosis. 2010; 210:71–77. [PubMed: 20226460]
53. Xu ZR, Hu L, Cheng LF, Qian Y, Yang YM. Dihydrotestosterone protects human vascular endothelial cells from H_2O_2-induced apoptosis through inhibition of caspase-3, caspase-9 and p38 MAPK. Eur J Pharmacol. 2010; 643:254–259. [PubMed: 20599910]

Appendix A. Supplementary data

Supplementary data to this article can be found online at doi:10. 1016/j.freeradbiomed. 2011.07.004.

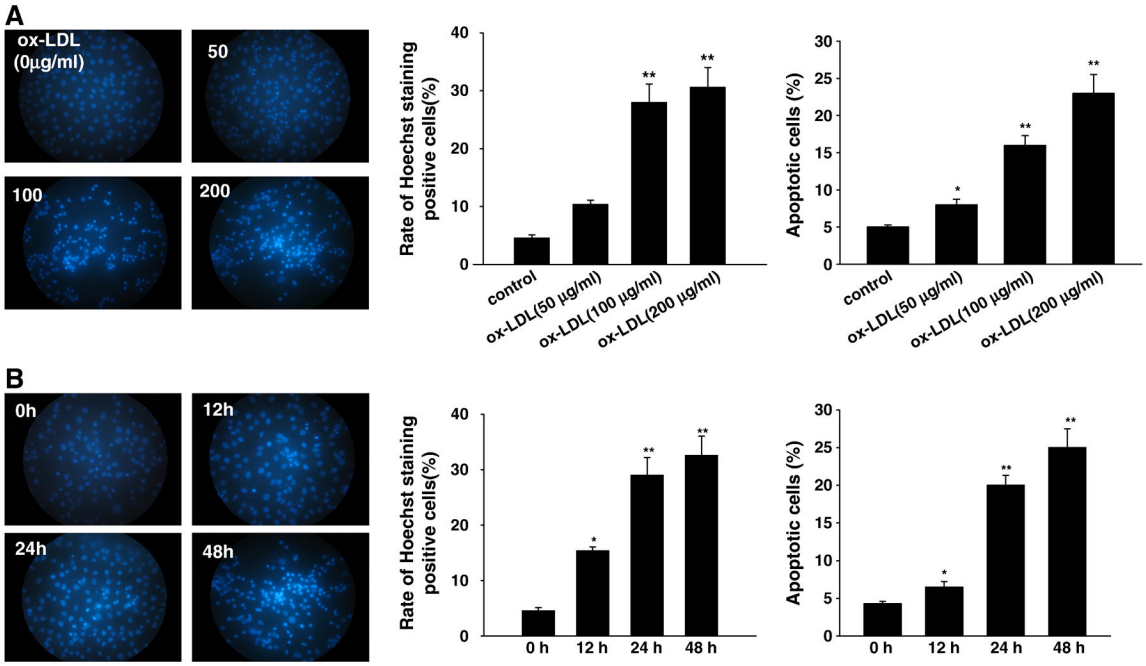

Fig. 1.

(A) Concentration response and (B) time course of ox-LDL-induced apoptosis in cultured HUVECs. (A) The endothelial cells were exposed to ox-LDL at various concentrations (50, 100, and 200 μg/ml) for 24 h. (B) The cells were exposed to ox-LDL (100 μg/ml) for 0, 12, 24, and 48 h. Apoptosis was determined by Hoechst 33342 staining and annexin V–PI double-staining assay (flow cytometry). Data are expressed as means±SEM, n=6 each, performed in triplicate. Compared with control (0 μg/ml ox-LDL) or 0 h, *P<0.05; **P<0.01.

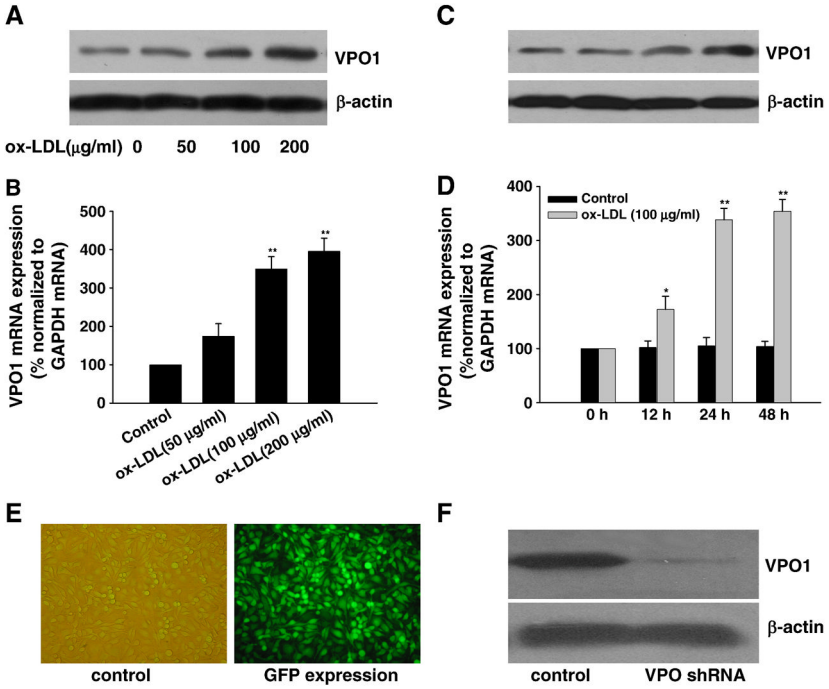

Fig. 2.

Expression of VPO1 in response to ox-LDL in HUVECs and effect of knockdown of VPO1 by shRNA. (A, B, C and D) Ox-LDL up-regulated the expression of VPO1 (both mRNA and protein, analyzed by real-time PCR and Western blot, respectively) in a time- and concentration-dependent manner. (E) GFP immunofluorescence staining of the cells transfected with VPO1-shRNA. (F) VPO1-shRNA successfully decreased VPO1 protein expression. Data are expressed as means±SEM, n=6 each, performed in triplicate. Compared with control (0μg/ml ox-LDL) or 0 h, *P<0.05; **P<0.01.

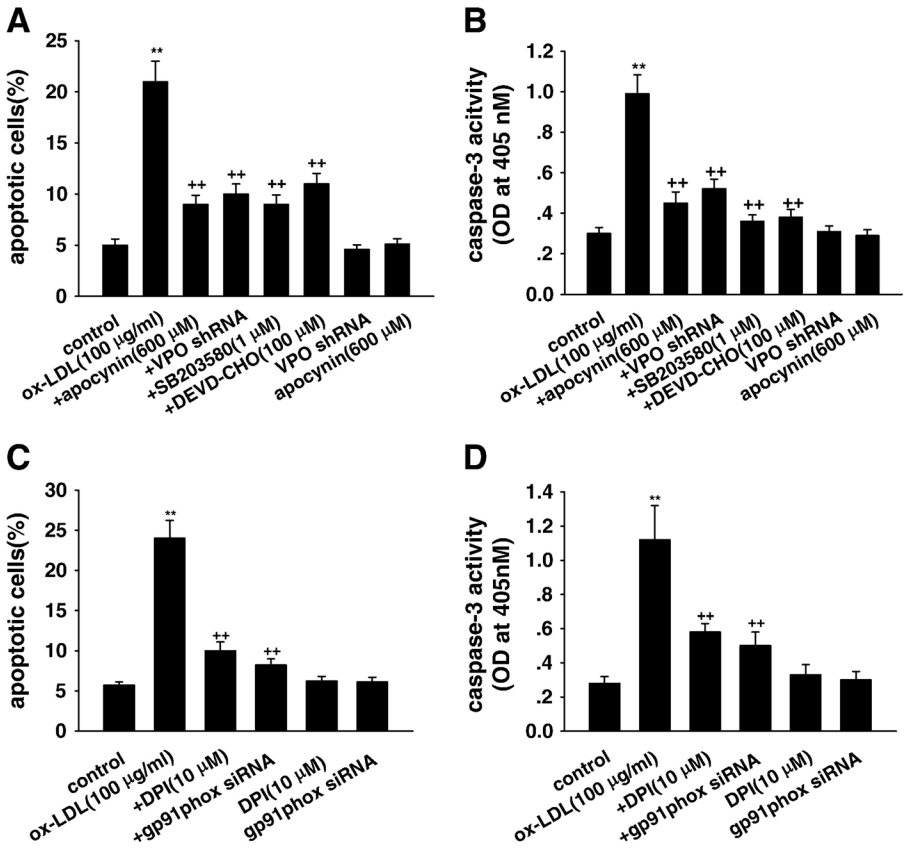

Fig. 3.

Effects of VPO1 knockdown on apoptosis of HUVECs induced by ox-LDL. (A and C) Cell apoptosis analysis by flow cytometry. (B and D) Caspase-3 activity. Control, wild-type cells were treated with 0 μg/ml ox-LDL for 24 h; ox-LDL, wild-type cells were treated with 100 μg/ml ox-LDL for 24 h; +DPI, cells were pretreated with 10 μM DPI (the specific NADPH oxidase inhibitor) for 1 h before ox-LDL exposure; +apocynin, cells were pretreated with 600 μM apocynin for 1 h before ox-LDL exposure; +gp91^{phox} siRNA, after successful gp91^{phox} siRNA transfection, cells were cultured in DMEM containing 100 μg/ml ox-LDL for 24 h; +VPO shRNA, after successful VPO1 shRNA transfection, cells were cultured in DMEM containing 100 μg/ml ox-LDL for 24 h; +SB203580, cells were pretreated with 1 μM SB203580 (the specific p38 MAPK inhibitor) for 1 h before ox-LDL exposure; +DEVD-CHO, cells were pretreated with 100 μM DEVD-CHO (the specific caspase-3 inhibitor) for 1 h before ox-LDL exposure; gp91^{phox} siRNA, cells with successful gp91^{phox} siRNA transfection were incubated in DMEM containing 1% calf serum for 24 h; VPO shRNA, cells with successful VPO1 shRNA transfection were incubated in DMEM containing 1% calf serum for 24 h; DPI, cells were cultured in DMEM containing 10 μM DPI for 24 h; apocynin, cells were cultured in DMEM containing 600 μM apocynin for 24 h. $^{**}P<0.01$ vs control (0 μg/ml ox-LDL), $^{++}P<0.01$ vs ox-LDL (100 μg/ml). Data are expressed as means±SEM, $n=6$ each, performed in triplicate.

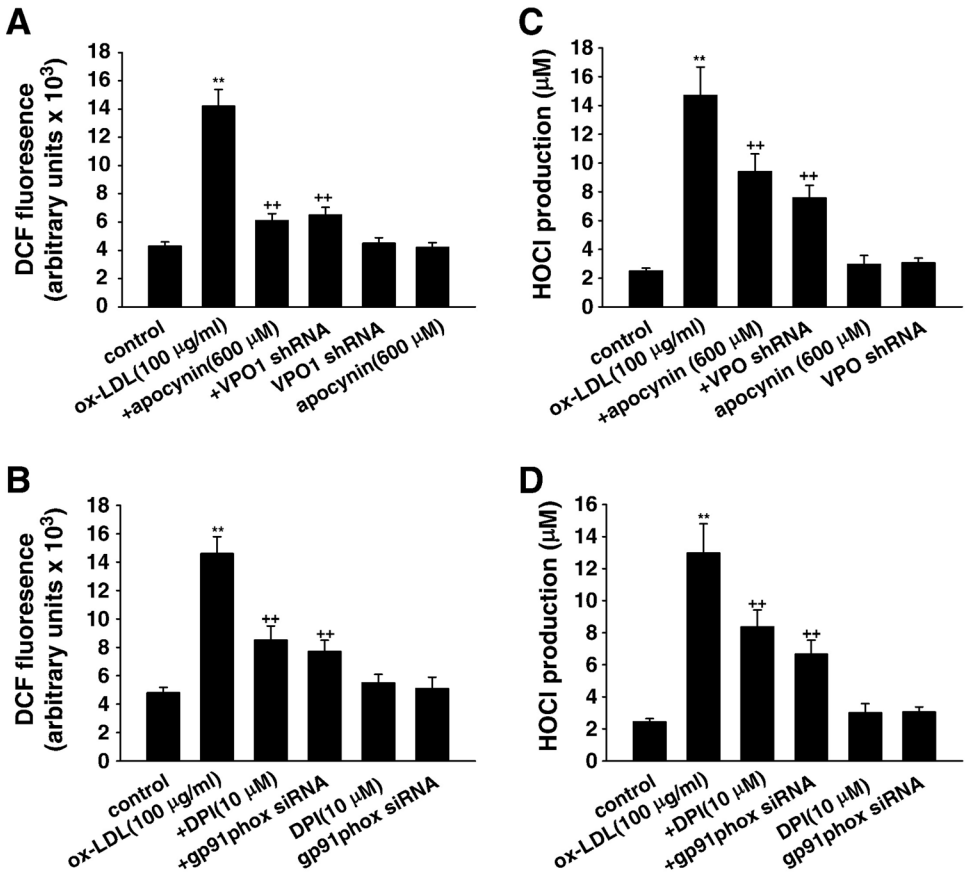

Fig. 4.

The role of intracellular ROS and HOCl in ox-LDL-induced apoptosis in HUVECs. (A and B) Intracellular ROS level was determined by fluorescent DCF. (C and D) HOCl production was determined by TMB assay. Control, wild-type cells were incubated in 10 mM phosphate buffer containing 5 mM taurine for 30 min; ox-LDL (100 μg/ml), wild-type cells were cultured in 10 mM phosphate buffer containing 5 mM taurine and ox-LDL (100 μg/ml) for 30 min; +DPI, cells were pretreated with 10 μM DPI (the specific NADPH oxidase inhibitor) for 1 h before ox-LDL exposure; +apocynin, cells were pretreated with 600 μM apocynin for 1 h before ox-LDL exposure; +gp91^{phox} siRNA, after successful gp91^{phox} siRNA transfection, cells were cultured in 10 mM phosphate buffer containing 5 mM taurine and ox-LDL (100 μg/ml) for 30 min; +VPO shRNA, after successful VPO1 shRNA transfection, cells were cultured in 10 mM phosphate buffer containing 5 mM taurine and ox-LDL (100 μg/ml) for 30 min; gp91^{phox} siRNA, cells with successful gp91^{phox} siRNA transfection were incubated in 10 mM phosphate buffer containing 5 mM taurine for 30 min; VPO shRNA, cells with successful VPO shRNA transfection were incubated in 10 mM phosphate buffer containing 5 mM taurine for 30 min; DPI, cells were cultured in 10 mM phosphate buffer containing 5 mM taurine and 10 μM DPI for 30 min; apocynin, cells were cultured in 10 mM phosphate buffer containing 5 mM taurine and 600 μM apocynin for 30 min. $^{**}P<0.01$ vs control (0 μg/ml ox-LDL), $^{++}P<0.01$ vs ox-LDL (100 μg/ml). Data are expressed as means±SEM, $n=6$ each, performed in triplicate.

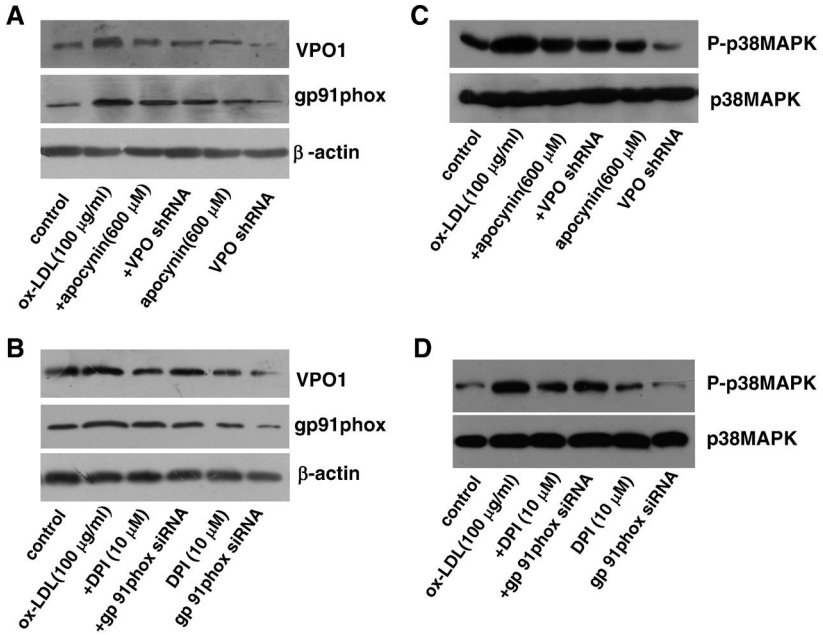

Fig. 5.

Relationship between VPO1 and the NADPH oxidase/p38 MAPK pathway in ox-LDL-induced apoptosis in HUVECs. (A and B) The protein levels of VPO1 and NADPH oxidase subunit gp91^{phox}. (C and D) The protein levels of (phosphorylated) p38 MAPK. Control, endothelial cells were incubated in DMEM containing 1% calf serum for 24 h; ox-LDL (100 μg/ml), endothelial cells were cultured in DMEM containing 100 μg/ml ox-LDL for 24 h; +DPI, cells were pretreated with 10 μM DPI (the specific NADPH oxidase inhibitor) for 1 h before ox-LDL exposure; +apocynin, cells were pretreated with 600 μM apocynin for 1 h before ox-LDL exposure; +gp91^{phox} siRNA, after successful gp91^{phox} siRNA transfection, cells were cultured in DMEM containing 100 μg/ml ox-LDL for 24 h; +VPO shRNA, after successful VPO1 shRNA transfection, cells were cultured in DMEM containing 100 μg/ml ox-LDL for 24 h; gp91^{phox} siRNA, cells with successful gp91^{phox} siRNA transfection were incubated in DMEM containing 1% calf serum for 24 h; VPO shRNA, cells with successful VPO1 shRNA transfection were incubated in DMEM containing 1% calf serum for 24 h; DPI, cells were cultured in DMEM containing 10 μM DPI for 24 h; apocynin, cells were cultured in DMEM containing 600 μM apocynin for 24 h. n=6 each, performed in triplicate.

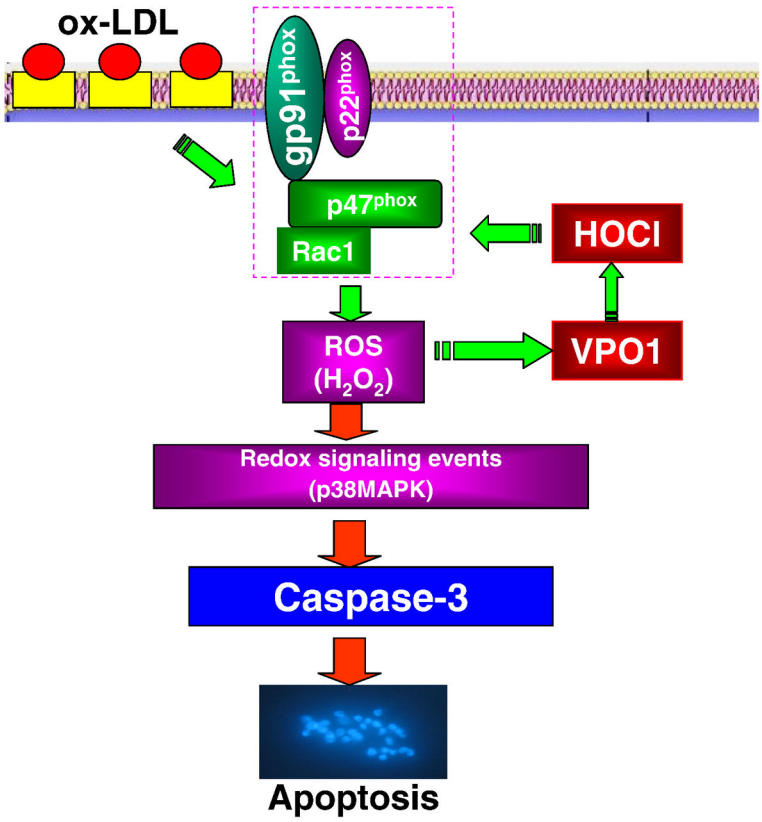

Fig. 6.

The proposed pathway of VPO1 mediation of ox-LDL-induced endothelial cell apoptosis. Ox-LDL up-regulates the expression of NADPH oxidase subunit $gp91^{phox}$ and consequently increases intracellular ROS production and VPO1 expression as well as HOCl production. There is a positive feedback loop between VPO1/HOCl and the NADPH oxidase/ROS pathway, which in turn activates the p38 MAPK/caspase-3-dependent signaling pathway to mediate ox-LDL-induced endothelial cell apoptosis.